

Received 3 May 2024, accepted 14 May 2024, date of publication 20 May 2024, date of current version 28 May 2024.

Digital Object Identifier 10.1109/ACCESS.2024.3402676

APPLIED RESEARCH

Pre-Accreditation With a Unified Coil for Radiated Interference Between Unspecified Balises and Railway Traction Inverters

SATORU HATSUKADE^{1,2}, (Member, IEEE), AND KEIJI WADA², (Senior Member, IEEE)

¹Vehicle Technology Division, Railway Technical Research Institute, Kokubunji, Tokyo 185-8540, Japan

²Graduate School of Systems Design, Tokyo Metropolitan University, Hino, Tokyo 192-0397, Japan

Corresponding author: Satoru Hatsukade (hatsukade@mem.iee.or.jp)

ABSTRACT Modern electric railway vehicles are faced with the challenge of achieving electromagnetic compatibility (EMC) compliance with railway signaling systems. Currently, no established countermeasures or design methods that guarantee passing the EMC compliance test are available. Therefore, the enhancement of EMC management during vehicle manufacturing processes is imperative. This study devised a pre-accreditation method to be implemented at the vehicle completion stage, prior to the EMC compliance test. The proposed method entails the substitution of real ground signaling devices, whose parameters are difficult to obtain, with unified coils. The effectiveness of this approach is validated by observing whether the gain difference remains consistent when using both an exciting coil and a test train. To illustrate this method, we selected the platform screen door (PSD) balise as a representative signaling device, which is widely utilized in various railway stations. The unified coil employed in this study can be easily fabricated. First, we measured the gain difference (the ratio between the induced voltage of coils and the exciting coil current) between the PSD balise and unified coil. Next, we measured the unknown magnetic flux induced by an 8-car electric multiple unit test train by utilizing the PSD balise and unified coil. Finally, we calculated the measured difference between them. The gain and measured differences properly agreed (within 6 dB) across a wide frequency range of 200 kHz to 4 MHz.

INDEX TERMS Electromagnetic measurements, electromagnetic radiative interference, inverters, magnetic field measurement, rail transportation, railway engineering.

I. INTRODUCTION

Reducing electromagnetic interference (EMI) in railway signaling equipment is crucial owing to the emission of unwanted electromagnetic waves by traction or auxiliary power converters on rolling stocks [1], [2], [3], [4]. Recently, the utilization of SiC semiconductors in railway vehicles has become prevalent [5], [6], resulting in radiated electromagnetic waves of higher frequencies from these vehicles.

The associate editor coordinating the review of this manuscript and approving it for publication was Chi-Seng Lam¹.

Consequently, these inverters must comply with the limits set by the IEC 62236 (EN 50121) series and satisfy the requirements of various railway signaling devices in the intended operating environment [7], [8], [9], [10], [11], [12].

The impact of electromagnetic waves on ground signaling devices has shifted from beacons or axle counters [13], [14] to devices known as “balises” or “transponders” [15], [16], [17], [18], [19], [20], [21]. Beacons or axle counters typically operate at several tens of kHz as they transmit only a few bits of information. However, balises or transponders operate at several MHz to accommodate higher bitrate. For example,

Japanese transponders operate at frequencies of 1.7 MHz and 3 MHz, whereas Eurobalise operates at 4.5 MHz, which can be influenced by the power converter's higher switching frequency.

The significance of EMC problems between rolling stock and railway signaling systems has been highlighted in numerous studies [1], [2], [3]. Such problems, stemming from fail-safe design principles, often lead to interruptions in communications with balises or transponders. This interference halts train operations, resulting in cancellations and considerable delays. Furthermore, certain signaling systems that determine train speeds by capturing beacon signals can underestimate these speeds owing to electromagnetic interference (EMI), thereby increasing the risk of train collisions [22].

Recently, balises have been utilized in communication to interlock the opening/closing of platform screen door (PSD) systems. These PSD balises are crucial in detecting whether a train has stopped within the permissible area of the PSD. As the permissible area varies depending on the railway infrastructure company, each PSD balise must be tailored to fit the length requirements of the permissible area. Therefore, the number of balise types subject to electromagnetic compatibility (EMC) testing has doubled, increasing the risk of failure in EMC tests.

Increasing the frequencies in balises could potentially alleviate EMC issues. However, owing to the widespread installation of signaling devices along operational lines, the cost of replacement is prohibitively high. Consequently, once installed, these devices typically remain in use for over 50 years. During this period, the switching frequency of traction inverters is likely to continue rising, perpetuating the EMI problem and rendering it unsolvable.

EMC chambers are a standard solution for conducting EMC tests. However, considering a 10-car train stretches up to 200 m in length, accommodating such a sizable train within an EMC chamber is unfeasible. While it is possible to measure emissions from a single traction inverter in compliance with IEC 62236-3-2 within an EMC chamber, these results do not accurately predict the impact on signaling equipment. This discrepancy arises because testing a solitary inverter does not replicate the complex installation environment found within a vehicle.

Therefore, various measurements [23], [24], [25], [26], [27], [28], [29], analyses [30], [31], [32], [33], [34], [35], [36], [37], [38], [39], and countermeasures [40], [41], [42], [43], [44], [45] have been proposed for rolling stock EMC. Currently, no established design or manufacturing method exists that can guarantee acceptance for all types of signaling systems. Thus EMC management must be enhanced [46], [47], [48] in the rolling stock manufacturing process. In particular, a pre-test or pre-accreditation is required in the manufacturing process. These pre-checks involve evaluating common-mode (CM) currents, which are the primary source of radiated electromagnetic fields, through simulations [43], [49], [50] or measurements [51], [52], [53], [54]. However, these pre-checks have limitations owing to unknown circuit

parameters in the design or manufacture of the power converters. Moreover, the effectiveness of this method is significantly reduced at frequencies above 1 MHz, which are utilized in balises, owing to changes in the current path caused by stray capacitances in the rolling stock.

To mitigate these issues, in this study, we devised a pre-accreditation method that can estimate the pass or fail outcome of EMC tests immediately after the installation of power converters in the vehicle. Furthermore, we examined the effectiveness of this pre-accreditation method. The proposed method utilizes a unified coil with clear specifications (310 mm wide and 430 mm long) that can be easily fabricated. The validation of the pre-accreditation is based on whether the difference between the values measured by utilizing a ground signaling device and the unified coil can be quantitatively determined. A PSD balise with unknown parameters was employed as a representative railway signaling device. A real train (an 8-car train) was also used in this study for generating unknown magnetic flux.

First, we calculated the gain difference between the PSD balise and unified coil. The gain refers to the measured ratio between the induced voltage and current in an exciting coil (1 m × 1 m square shape, 1-turn coil). Next, we measured the unknown magnetic field generated by an 8-car train using the PSD balise and unified coil and calculated the measured difference between them. Finally, we validated that the gain differences obtained by utilizing the exciting coil and that measured by utilizing the test train were in good agreement. This agreement implies that the EMC limits of ground signaling systems can be effectively converted to the limits of the unified coil, thus making pre-accreditation a viable option.

The proposed pre-accreditation method offers several distinct advantages. First, it can be executed without knowledge of the internal parameters, such as coil windings or circuit parameters, in the connected receiver. Additionally, the pre-accreditation approach enables the testing of multiple types of signaling devices using a single unified coil.

II. PRE-ACCREDITATION USING A UNIFIED COIL

A. CONCEPT

The overall concept of the pre-accreditation utilized in this study is shown in Fig. 1. To simulate ground signaling devices, we employed a unified coil with a known size and termination resistance. By establishing a quantitative correlation between the unified coil and ground signaling devices, we can convert the EMC limits of the ground signaling devices to those of the unified coil. In this study, we consider transponders [18], which are commonly utilized as ground elements and cover a center frequency (CF) range of 1 MHz to 4 MHz.

B. QUANTITATIVE RELATIONSHIP BETWEEN AN ACTUAL BALISE AND A UNIFIED COIL

1) GAIN MEASUREMENT OF THE EXCITING COIL

Owing to confidentiality concerns, detailed parameters are often not disclosed. Therefore, we need an additional

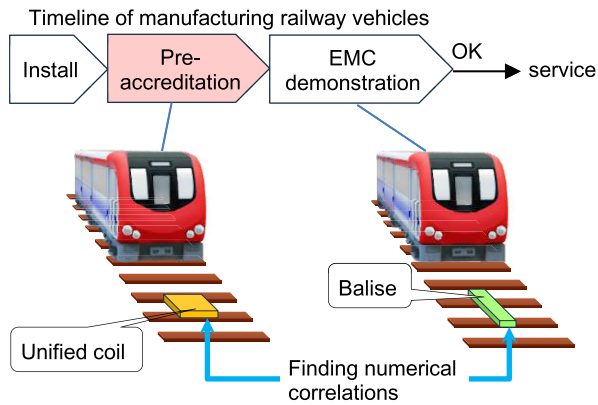


FIGURE 1. Proposed concept of pre-accreditation.

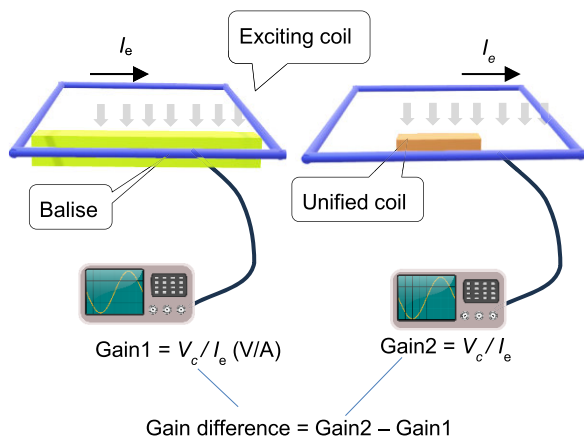


FIGURE 2. Gain measurements of the unified coil and balise.

parameter to establish a quantitative correlation. In this study, we utilize gain (V/A) between the induced voltage V_c of the exciting coil and the coil current I_e as shown in Fig. 2. The purpose of the exciting coil is to generate a uniform magnetic field. By separately measuring the gain for the PSD balise and unified coil, we can determine the gain difference between the two. This gain difference allows for the conversion of the EMC limits of the PSD balise to the limits of the unified coil.

For the exciting coil, we employed a 1-turn coil with a square shape (1 m × 1 m) as shown in Fig. 2. The size of the exciting coil is specified in the Japanese Industrial Standard (JIS) E 3004. Similar exciting coils have been utilized in some studies [55], [56] to determine the immunity of railway signaling devices. The assembly and setup of the exciting coil utilized in this study are shown in Fig. 3. The displacement between the exciting coil and coil under test (CUT) was 10 cm, following the guidelines outlined in the JIS standard. The exciting coil was fabricated of aluminum and utilized assembled parts of the luggage racks, enabling convenient on-site assembly (Table 1).

Based on the analysis results [56], the magnetic field strength generated by the exciting coil was 1.6 mA/m per 1 mA of the exciting coil current. The results were validated using the free software [56], as shown in Fig. 4. Notably,

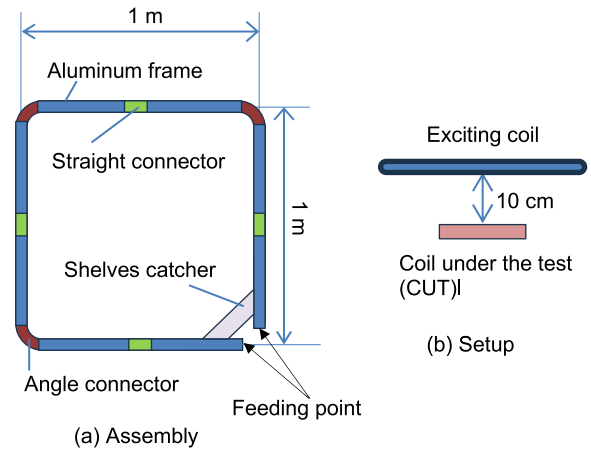


FIGURE 3. Exciting coil assembly and its setup.

TABLE 1. Parts of the exciting coil.

Parts	Vender	Item code	No. of items
Aluminum frame	Misumi	GFF-400/L473	8
Angle connector	Misumi	GFJ-046	3
Straight connector	Misumi	GFJ-089	4
Shelves catch	Misumi	VPJ-700B	1

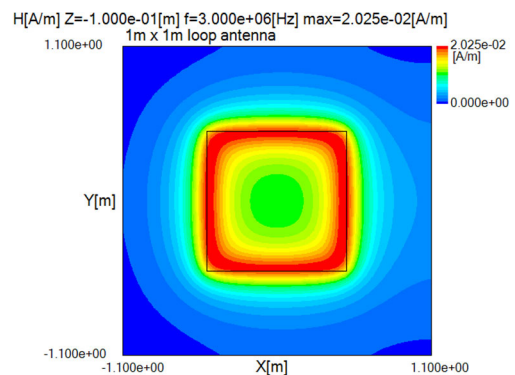


FIGURE 4. Numerical result of the magnetic flux from the exciting coil.

OpenTHFD can only utilize voltage sources; thus, the coil current in Fig. 4 is 12.52 mA at 3 MHz. By converting this result, we can obtain a value of 1.62 mA/m per 1 mA. The result at 100 kHz was calculated as 1.70 mA/m, indicating no frequency dependence.

2) UNIFIED COIL

The unified coil shown in Fig. 5 was utilized in this study. For high-frequency measurements, a smaller coil size is preferred. However, for accreditation, it's important that the coil's shape closely resembles that of an actual PSD balise. In Japan, the maximum width of PSD balises along the sleeper direction is 310 mm, and their length in the rail direction can exceed 1 m in certain instances. Thus, the unified coil described in this study is designed with dimensions of 310 mm in width and 420 mm in length. This size not only accommodates the majority of PSD balises in Japan but also

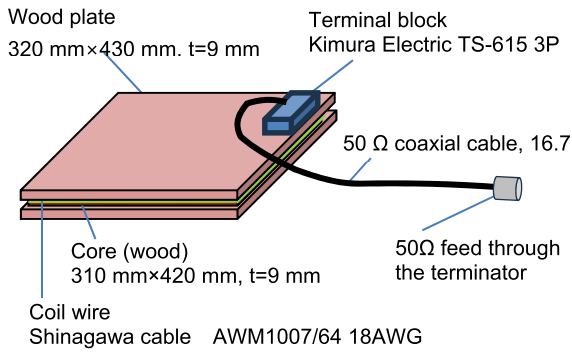


FIGURE 5. Unified coil assembly, cabling, and termination.

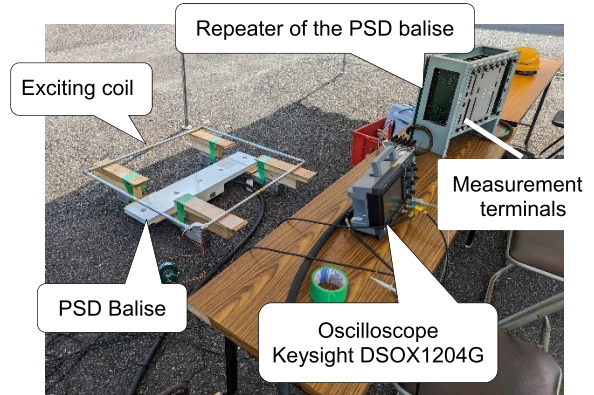


FIGURE 8. Photograph of the gain measurement of the PSD balise.

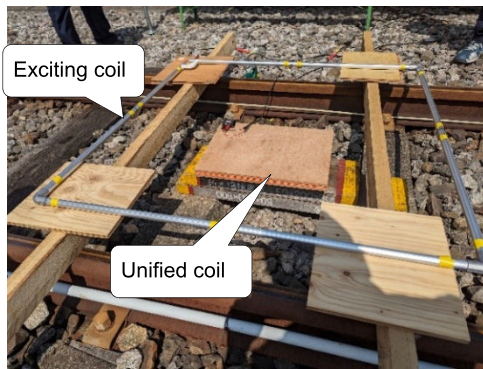


FIGURE 6. Photograph of the gain measurement of the unified coil.

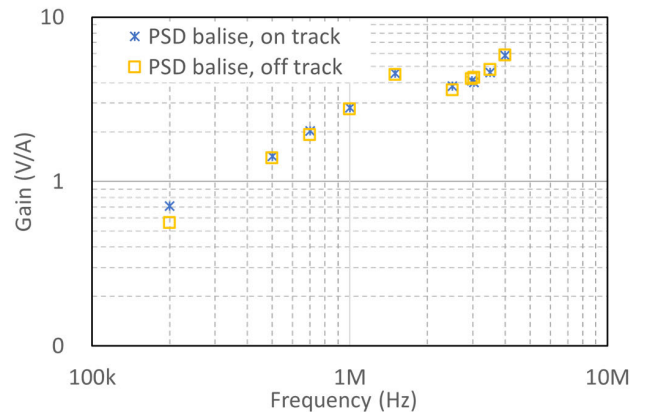


FIGURE 9. Gain of the PSD balise.

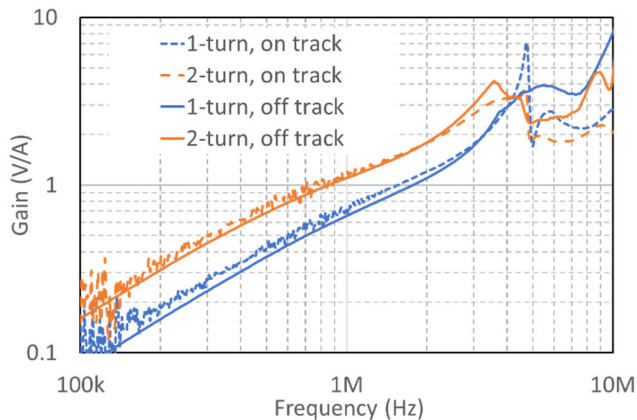


FIGURE 7. Gain of the unified coils.

TABLE 2. Gain difference using the exciting coil.

Frequency (kHz)	Gain differences between the unified coil and PSD balise, out of track (dB)	
	1-turn	2-turn
200	-10.95	-5.06
500	-11.45	-6.16
700	-11.79	-6.87
1000	-12.48	-7.93
1500	-13.93	-9.86
2500	-8.47	-3.92
2968	-7.86	-2.88
3500	-6.49	-1.54
4000	-6.09	-4.46

ensures ease of handling. In addition, to ensure repeatability during fabrication and prevent self-resonance, the coil was terminated with a 50 Ω resistor. Two types of turns (one and two) were utilized in this study.

A photograph of the gain measurement of the unified coil using the exciting coil on the track is shown in Fig. 6, whereas the measurement results are shown in Fig. 7. We achieved a gain of 0.6 V/A or better from 1 MHz to 10 MHz. In addition, the measurement results under the on-track and off-track conditions were almost identical between 100 kHz and 5 MHz. This indicates that the gain measurements were not influenced by the rail or track. However, deviations were observed at frequencies above 5 MHz, which resulted from

the self-resonance of the unified coil and the effect of the probe capacitance.

3) GAIN DIFFERENCE BETWEEN THE PSD BALISE AND UNIFIED COIL

Fig. 8 displays a photograph capturing the gain measurement of a PSD balise that has been displaced from its track. This balise is equipped with multiple coils, serving not only to facilitate the transmission and reception of signals to and from platform doors but also to ascertain the precise stopping positions of trains. The PSD balise uses 3 MHz in receiving and 1.7 MHz in transmitting. Moreover, the PSD



FIGURE 10. Test train (Tokyo Metro Series 9000).

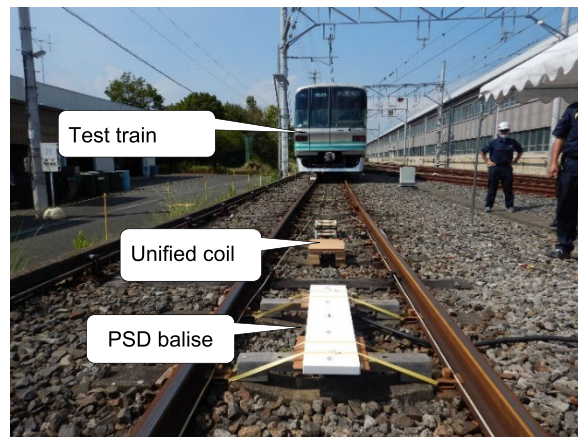


FIGURE 12. Photograph of the test site.

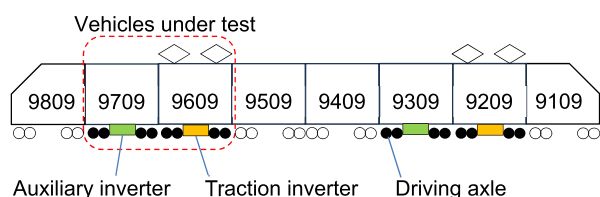


FIGURE 11. Details of the test train.

TABLE 3. Specification of the test train.

Formation	8 cars (4 power cars, 4 trailers)
Manufacture year	1995
Refurbished year	2023
Track gauge	1067 mm
Electric system	Overhead line, 1.5 kV DC
Maximum speed	110 km/h
Traction system	Traction inverter + 225 kW 3-phase AC induction motor
Power semiconductors	Traction inverter: SiC FET + SiC Di Auxiliary inverter: Si IGBT + SiC Di

balise is connected to its repeater whose parameters are unknown. Consequently, the gain characteristic of the PSD balise is not monotonous, unlike that of the unified coil. The gain characteristics of the receiver coil of the PSD balise is shown in Fig. 9. The discrete nature of the graph results from the manufacturer’s confidentiality regarding the detailed characteristics.

The gain differences between the unified coil and PSD balise from Figs. 7 and 9 are presented in Table 2. This value is referred to as the “exciting coil” in the figures and hereinafter. Further, the value is employed to check whether the gain difference caused by the exciting coil is equivalent to that caused by the test train.

III. VALIDATION OF NUMERICAL CORRELATIONS BETWEEN THE PSD BALISE AND UNIFIED COIL USING THE TEST TRAIN

In the previous section, we measured the difference in gain between the PSD balise and the unified coils using an excitation coil. Here, we aim to validate whether the difference

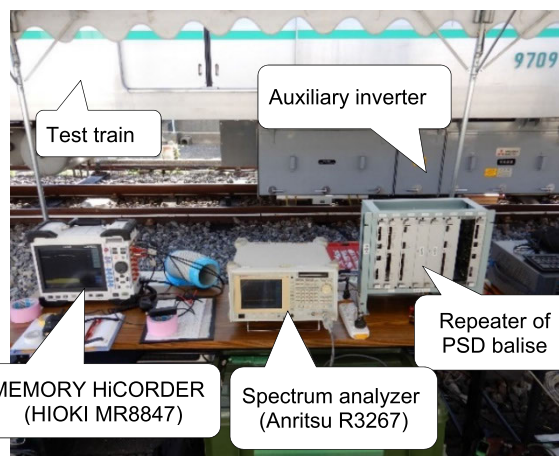


FIGURE 13. Measurement setup for the PSD balise, similar to that of the EMC compliance test.

in gain obtained with the excitation coil can be reproduced in measurements conducted on real vehicles. For this purpose, we utilized a test train, as shown in Figs. 10 and 11, with detailed specifications listed in Table 3. An 8-car subway train that operates on 1500 Vdc overhead lines and is equipped with a traction inverter on Car 9609 was utilized as the test train. Car 9709 was equipped with an inverter as an auxiliary power source. We measured the magnetic fields emitted by these inverters and cabling using the PSD balise or unified coil.

Testing was conducted in a test track at a train depot in Tokyo Metropolis (Fig. 12). On this test track, a maximum speed of 25 km/h was recorded on a drivable section of approximately 300 m.

A. VALIDATION OF THE EMC COMPLIANCE TEST METHOD

This section examines the validation results obtained under the same measurement setup as that of the EMC compliance test for the PSD balise. The setup is shown in Fig. 13. The measurement point was the repeater terminal connected to the PSD balise. The spectrum analyzer shown in Fig. 13 was set to the zero-span mode with a CF of 2968 kHz and a resolution

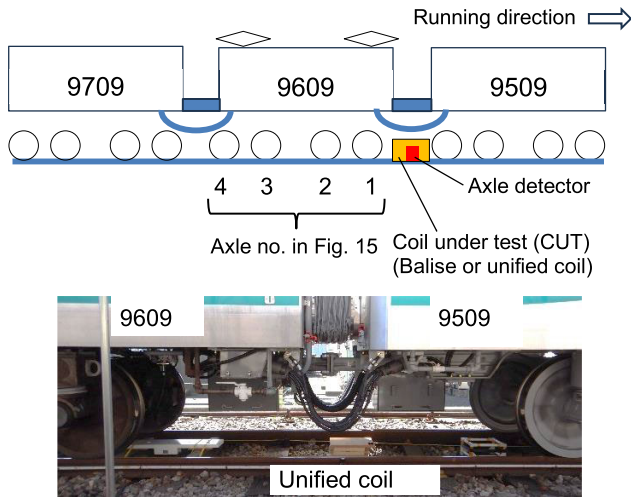


FIGURE 14. Starting position in the powering test.

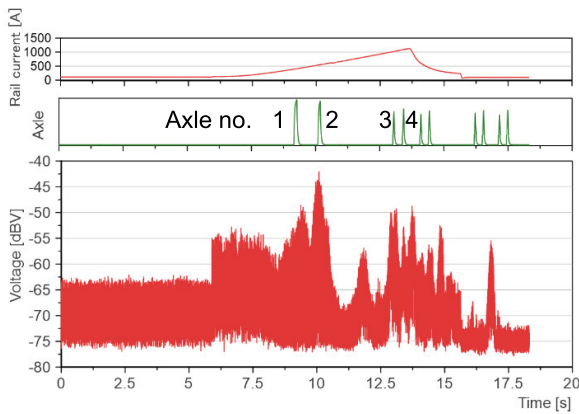


FIGURE 15. Example chart from the powering test (Memory HiCORDER).

bandwidth (RBW) of 30 kHz. Additionally, we employed a recorder (MEMORY HiCORDER, shown in Fig. 13) to capture the video output of the spectrum analyzer, enabling the creation of time-axis waveforms. The recorder also recorded the axle detector (Fig. 14) and the rail current to monitor the status of the test train. The rail current was derived from the measured voltage between the two points on the rail, with the driver’s cab display serving as the reference value.

The tests conducted on the CUT, which include the PSD balise, 1-turn unified coil, and 2-turn unified coil, can be categorized into four: auxiliary inverter test, stationary test, powering, and braking. During the auxiliary inverter test, measurements are obtained for approximately 5 min from the start to the stop of the auxiliary inverter. Within this measurement period, the loads of the auxiliary inverter, such as air conditioners, were switched ON and OFF. In the stationary test, the test train was stopped at the position where the radiation was expected to be maximum. During this test, the traction inverter operated for a few seconds.

The starting position of the powering test is shown in Fig. 14. During the braking test, the test train started from the end of the test site (the relationship between the test train

TABLE 4. Peak values for a setup similar to that of the compliance test.

CUT	PSD balise (dBV)	1-turn unified coil (dBV)	2-turn unified coil (dBV)
Auxiliary inverter	-58.0	-63.3	-58.0
Stationary test (powering)	-53.0	-52.7	-54.3
Powering	-43.0	-49.1	-44.7
	-42.2	-48.2	-42.4
Braking (regenerative)	-42.1	-48.8	-43.5
	-41.9	-48.0	-41.7
	-47.6	-47.5	-42.0
	-46.5	-47.4	-43.9

TABLE 5. Gain difference between the PSD balise and unified coil.

	1-turn		2-turn	
	Train (dB)	Exciting coil (dB)	Train (dB)	Exciting coil (dB)
Aux. converter from start to stop	-5.30	-7.86	-0.01	-2.88
Stationary test (powering)	0.31		-1.25	
Powering	Max. -6.14		-0.31	
Braking (regenerative)	Max. -5.52		0.21	

and CUT is similar to that shown in Fig. 12) and immediately braked in front of the CUT in the regenerative braking mode. During the powering and braking tests, measurements were performed from the start of the traction inverter to the end of the test train. The powering and braking tests were performed in triplicate.

An example chart of the recorder is shown in Fig. 15, according to which the axle numbers indicate the axles that pass over the detector, as shown in Fig. 14. As shown in Fig. 15, the maximum radiation was observed from the second axis of Car 9609, indicating that the CM current in the motor cable on the second axle was the primary source of radiation.

The peak values for each measurement are listed in Table 4. A deviation of 5 dB was observed in the braking test for the PSD balise owing to the regenerative load instability; however, other tests showed small deviations of 1–3 dB. The powering test consistently yielded the highest results among all test categories for each CUT.

To investigate the exciting source, we calculated the measured difference between the PSD balise and unified coil, as shown in Table 2. During the powering and braking tests, we selected the maximum value for comparison purposes. The comparison results between the difference measured by the test train and the gain difference measured by the exciting coil are listed in Table 5. The differences measured by the train for the 1-turn unified coil were approximately 2 dB higher than the gain difference measured by the exciting coil and 3 dB higher for the 2-turn unified coil. These findings

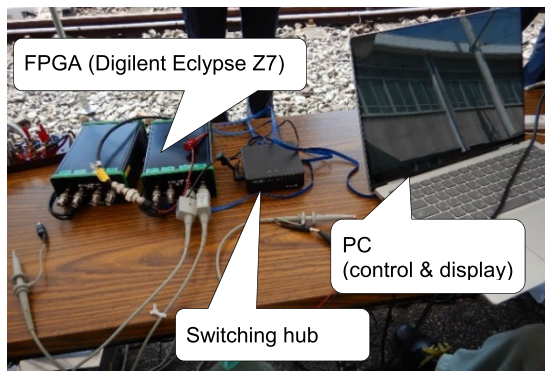


FIGURE 16. Octal input zero-span mode analyzer.

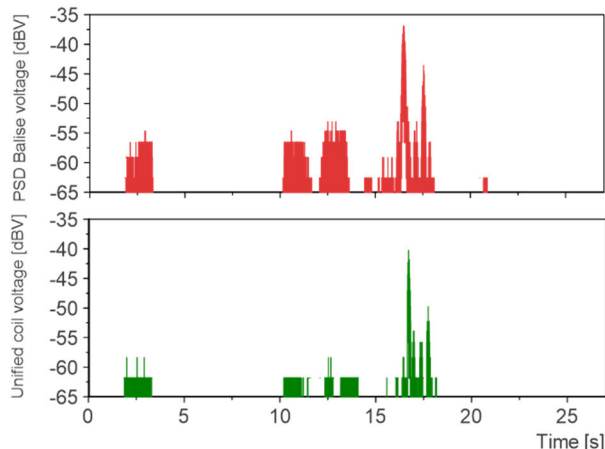


FIGURE 17. Example chart (octal input zero-span mode analyzer).

indicate that the gain difference was maintained between the unified coil and the test train. The fluctuation of 3 to 8 dB observed during the stationary test may be attributed to the difference in the stopping position of the test train.

B. VALIDATION MEASUREMENTS CONDUCTED BY SIMULTANEOUSLY UTILIZING TWO COILS

In the previous section, we conducted measurements at only one CF and could not perform simultaneous measurements for two coils. To address this limitation, we employed a measuring instrument, namely the octal input zero-span mode analyzer [58], as shown in Fig. 16. This instrument comprises a field-programmable gate array (FPGA) board (Digilent Eclipse Z7) equipped with two A/D converter boards (Digilent Zmod Scope 1410), offering four input channels per unit. One unit can simultaneously perform eight input measurements, equivalent to the zero-span mode of a spectrum analyzer. An example of the waveforms measured during the test train’s powering mode is shown in Fig. 17. As illustrated, the waveforms are correlated with the PSD balise and unified coil.

As explained in the previous section, we performed measurements using CUTs, and the maximum values are listed in Table 6. Notably, powering tests were performed to reduce the test time.

TABLE 6. Peak value measured at the same powering test (using an octal input zero-span mode analyzer).

CF, RBW (kHz)	PSD balise (dBV)	1-turn unified coil (dBV)	2-turn unified coil (dBV)
700, 10	-38.0	-46.2	-
	-38.5	-47.0	-
	-36.8	-46.2	-
1000, 10	-39.1	-46.2	-
	-37.0	-47.8	-
	-37.0	-45.6	-
2500, 30	-38.7	-44.2	-
	-38.1	-44.7	-
	-38.3	-45.2	-
2968, 30	-44.1	-49.3	-
	-44.5	-49.3	-
	-45.0	-50.2	-
4000, 30	-38.5	-45.8	-
	-38.1	-46.4	-
	-38.5	-44.7	-
1000, 10	-37.3	-	-41.0
	-36.8	-	-40.2
	-37.0	-	-41.0
2968, 30	-44.5	-	-43.7
	-43.3	-	-43.7
	-45.0	-	-45.2
4000, 30	-40.9	-	-42.5
	-38.3	-	-41.4
	-39.7	-	-43.3

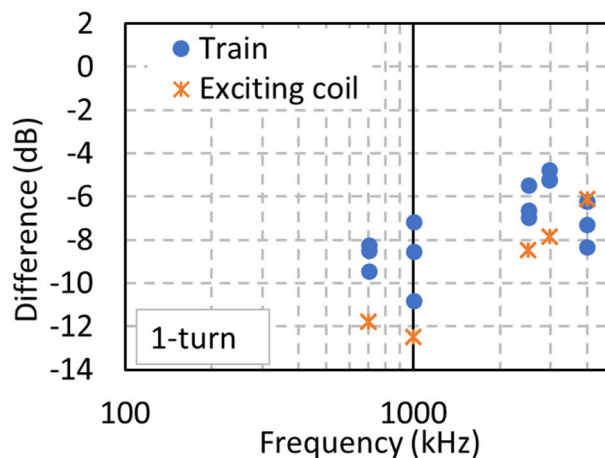


FIGURE 18. Gain difference of the 1-turn unified coil (octal input zero-span mode analyzer).

Because each row in Table 6 corresponded to one measurement, the measured differences between the PSD balise and unified coil could be calculated in each run. These differences, including the gain difference, are shown in Figs. 18 (1-turn coil) and 19 (2-turn coil). Compared with the gain difference measured by utilizing the exciting coil, the difference measured by utilizing the test train for the 1-turn unified coil deviated by a maximum of approximately 6 dB, whereas for the 2-turn coil, the difference deviated by a maximum of approximately 4 dB. Notably, the gain difference obtained by utilizing the exciting coil remained consistent in the

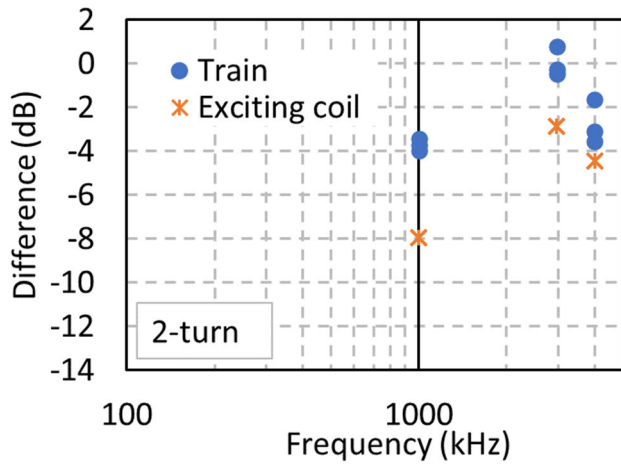


FIGURE 19. Gain difference of the 2-turn unified coil (octal input zero-span mode analyzer).

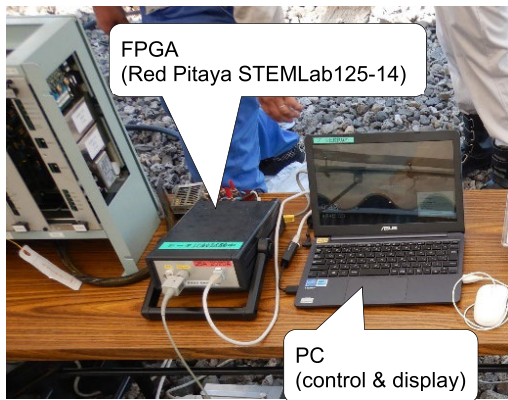


FIGURE 20. Quad frequency zero-span mode analyzer.

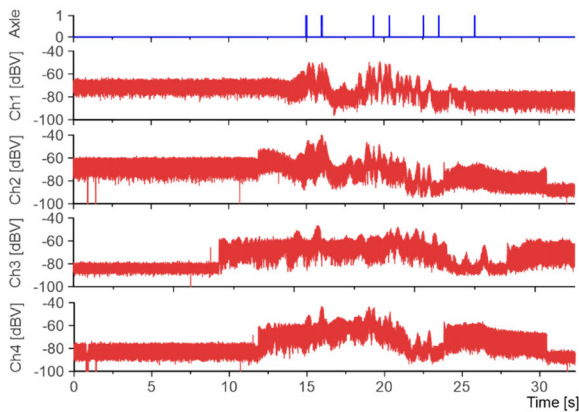


FIGURE 21. Example chart (quad frequency zero-span mode analyzer).

measurement performed by utilizing an actual vehicle, as explained in the previous section, considering the maximum variation of approximately 4 dB among the powering tests in Table 5.

C. VALIDATION OF THE MEASUREMENTS AT VARIOUS FREQUENCIES

Building upon the reproducibility of the measurements established in the previous section, this section aims to validate the

TABLE 7. Maximum and peak value fluctuations at various frequencies (using a quad frequency zero-span mode analyzer).

CF, RBW (kHz)	PSD balise		1-turn		2-turn	
	Max. (dBV)	Fluc. (dB)	Max. (dBV)	Fluc. (dB)	Max. (dBV)	Fluc. (dB)
200, 10	-47.90	0.88	-54.94	0.69	-48.07	1.57
500, 10	-45.34	0.30	-51.48	2.09	-53.43	2.18
700, 10	-36.98	1.16	-46.15	1.31	-47.46	0.85
1000, 10	-27.80	0.89	-36.93	0.20	-37.09	2.06
1500, 30	-32.26	0.24	-42.12	1.40	-43.26	0.99
2500, 30	-40.98	0.52	-46.59	0.53	-47.06	0.22
3500, 30	-46.43	0.57	-49.77	0.91	-50.46	1.96
4000, 30	-39.16	1.14	-46.27	1.22	-46.27	1.31

Fluc: Fluctuation

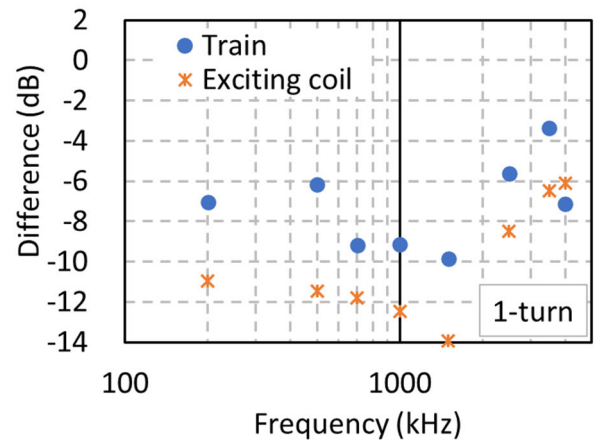


FIGURE 22. Gain difference for the 1-turn unified coil (Quad frequency zero-span mode analyzer).

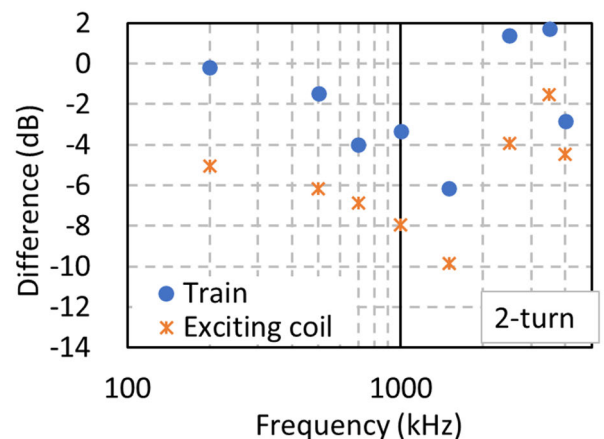


FIGURE 23. Gain difference for the 2-turn unified coil (quad frequency zero-span mode analyzer).

measurements at a wider range of CFs. The quad frequency zero-span mode analyzer was utilized as the measuring instrument in this section, as shown in Fig. 20. This instrument based on Red Pitaya STEMLab 125-14, an FPGA board with analog inputs, enables simultaneous zero-span mode measurements at four CFs. An example chart is shown in Fig. 21.

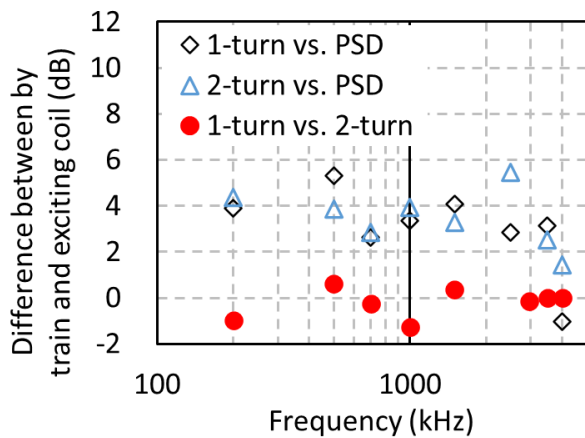


FIGURE 24. Difference between by train and by exciting coil (quad frequency zero-span mode analyzer).

For each CF and CUT, three powering tests were performed. The maximum and fluctuations in the peak values are listed in Table 7. Notably, the maximum fluctuation in this measurement was 2.2 dB, indicating a high level of reproducibility. The gain differences calculated from Table 7 for the 1-turn unified coil, as described in Section III-A and III-B are shown in Figs. 22 and 23. Comparing these results with those obtained by the exciting coil, the measured difference was within 3 to 6 dB for both 1-turn and 2-turn coils. Similar to the previous results, this consistency indicates that the gain difference obtained by utilizing the exciting coil at a CF ranging from 200 kHz to 4 MHz was maintained in the measurement obtained by utilizing the actual vehicle.

IV. DISCUSSIONS

A. GAIN DIFFERENCE OBTAINED BY UTILIZING THE EXCITING COIL AND TEST TRAIN

The gain differences observed between the test train and exciting coil, for both the 1-turn and 2-turn unified coils, as shown in Sections III-A, III-B, and III-C are noteworthy. This discrepancy can be attributed to the nature of the magnetic field generated. First, the exciting coil generates uniform magnetic fields. When using the exciting coil, the difference gain between the unified coils and the PSD balise is proportional to their coil area or the number of turns. The reason for the negative values in Figs. 18, 19, 22, and 23 is that the PSD balise, which has the largest area, is used as the reference (0 dB). On the other hand, Figs. 18, 19, 22, and 23 show that the gain difference by train is larger than that by the exciting coil. This means that the average magnetic field in the unified coils, which has a smaller area, is larger than that of the PSD balise when using train. It indicates that the magnetic field generated by the train is localized. It is also deduced from Fig. 24, which shows the difference between by train and by exciting among all coils. It highlights that the difference for coils of identical area but varying numbers of turns (1-turn vs. 2-turn) is smaller than the difference compared with the PSD balise.

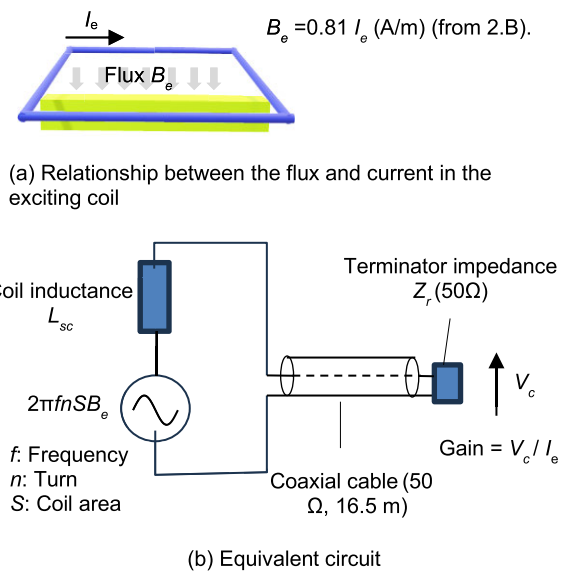


FIGURE 25. Gain calculation circuit.

TABLE 8. Calculation result of the gain from parameters (2968 kHz).

Parameters	1-turn coil	2-turn coil
Coil area S (m ²)	0.13	0.13
No. of turns	1	2
Coil impedance L _{sc} (μH)	1.69	6.77
Gain [V/A]	Calculated	2.00
	Measured	1.70
	Error (dB)	1.4

This finding also suggests that a smaller unified coil can be utilized as a substitute for a larger balise. Although a certain PSD balise may be 2 m long, the gain difference obtained by utilizing the unified coil and long PSD balise can be determined using the proposed method.

However, extremely long balises, such as those exceeding 10 m in length can cover magnetic fields from multiple motor cables. Consequently, the gain difference in such cases would significantly deviate from that observed with the unified coil. However, by examining the waveforms, we can determine whether the magnetic fields originate from multiple sources. Therefore, this scenario does not negate the effectiveness of pre-accreditation using a unified coil.

B. POSSIBILITY OF CALCULATING THE GAIN OF UNIFIED COILS USING CIRCUIT PARAMETERS

Suppose the gain for balises or unified coils can be calculated. In that case, the gain must not be measured using real devices. In some studies, the EMC limit for signaling devices was converted into the CM current limit using coil geometries and simple equivalent circuits of the receiver [51], [52]. This section explores the possibility of calculating the gain of the unified coils.

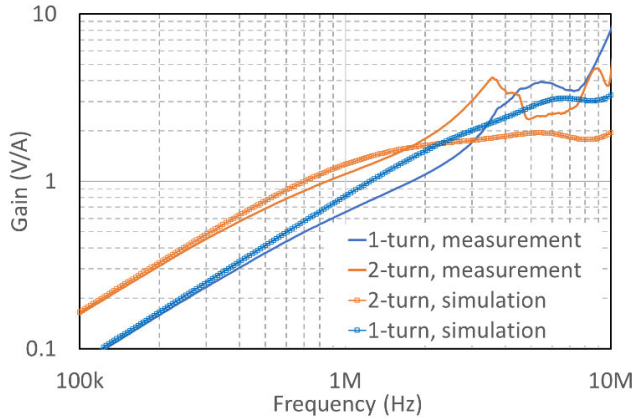


FIGURE 26. Gain calculation circuit.

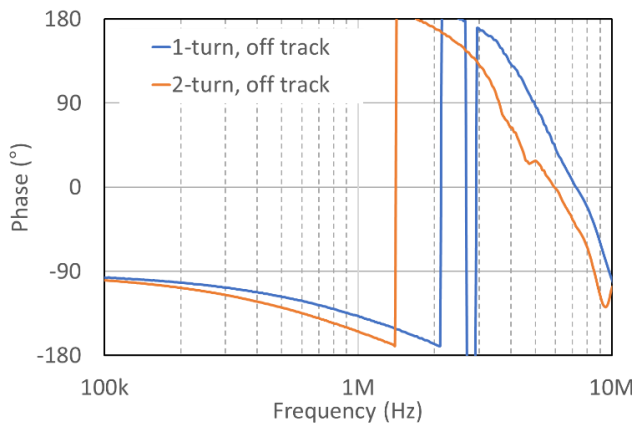


FIGURE 27. Measured phase between V_c and I_b in Fig. 7.

The equivalent circuit for measuring the gain V_c/I_e is shown in Fig. 25. In this circuit, the ratio of the magnetic field generated by the exciting coil's current was set to 0.81, based on the value at the center of the exciting coil as calculated in Section II-B (Fig. 4). The self-inductance was determined from the coil geometry. A comparison between the measurement and calculation results is shown in Table 8 and Fig. 26.

At the CF (2968 kHz) of the PSD balise, the calculated and measurement results for the 1-turn unified coil were almost consistent, whereas a discrepancy of approximately 5 dB was observed for the 2-turn unified coil. The gain characteristics shown in Fig. 26 indicate that frequencies above 700 kHz deviated from the two gains. This deviation was primarily caused by the rotation of the measured phase characteristics, as shown in Fig. 27, resulting from the 16.5 m coaxial cable. In rail depots, the distance between the test track and measurement site often exceeds 10 m on double-track systems, making it impractical to shorten the coaxial cable. Consequently, the gain characteristics of the PSD balise, as shown in Fig. 9, did not vary linearly with frequency. This nonlinearity poses challenges in calculating the gain based on the balise's parameters.

The proposed method offers a solution to eliminate uncertainties in specifications and equivalent circuits. Although

preliminary measurements on the actual device were required, our approach provided the advantage of converting the limits of the unified coil from any balise even if their internal parameters are completely unknown.

C. ACCREDITATION RESULT

The EMC limit for the PSD balise is set at -38 dBV by the manufacture of the PSD balise. The highest measurement reported in this study was -41.9 dBV, as detailed in Section III-A (Table 4), utilizing a setup identical to that of the final EMC compliance test. Four weeks following the measurements presented herein, the test train successfully passed the final EMC compliance test and has been operational in commercial service since December 16, 2023. With the capability to translate the EMC limit of the PSD balise into the equivalent for unified coils, pre-accreditation testing using these coils is now feasible.

V. CONCLUSION

This study developed a novel pre-accreditation method to enhance EMC management between rolling stock and signaling equipment. The proposed method utilized a unified coil, which can be easily fabricated, as a substitute for real signaling devices. In particular, a PSD balise was chosen as the representative railway signaling device. A real train (an 8-car train) was also used in validation.

The effectiveness of the pre-accreditation was validated by measuring the induced voltage difference between the real signaling device and unified coil under the same magnetic flux. This measurement was conducted using two magnetic sources: the exciting coil and an 8-car test train. To ensure accurate results, the validation measurements were performed at three different setups: similar to that of the EMC compliance test, simultaneous measurements using two coils, and measurements at various frequencies.

The validation results obtained from all measurement setups clearly demonstrated the effectiveness of pre-accreditation. The gain differences obtained by utilizing the exciting coil and those obtained by conducting measurements using the test train were within 6 dB in the frequency range of 200 kHz to 4 MHz. This outcome allowed for the conversion of the EMC limit for the unified coil from that of signaling devices.

The pre-accreditation method proposed in this study offered several advantages. It can be easily implemented by rolling stock manufacturers and facilitates the comparison of immunity levels among different types of balises.

The findings of this study are applicable up to 4 MHz, a limitation imposed by the large dimensions of the unified coils utilized. If balises used higher frequencies in the future, smaller unified coils would be more suitable, representing an area for future research.

ACKNOWLEDGMENT

The measurements in this study were performed as a part of activities of a working group (WG) established by Japan

Railway Rolling Stock and Machinery Association. The authors would like to express their gratitude to the members of the WG, particularly Tokyo Metro Company Ltd., Mitsubishi Electric Corporation, and Kyosan Electric Manufacturing Company Ltd., for their cooperation. They also would like to thank Editage (www.editage.jp) for English language editing.

REFERENCES

- [1] A. Ogunsola and A. Mariscotti, *Electromagnetic Compatibility in Railways: Analysis and Management*. Berlin, Germany: Springer, 2012.
- [2] F. R. Holmstrom, D. Turner, and E. Fernald, "Rail transit EMI-EMC," *IEEE Electromagn. Compat. Mag.*, vol. 1, no. 1, pp. 79–82, 1st Quart., 2012.
- [3] R. Holmes, "Electromagnetic compatibility of electrified railways," in *Proc. Int. Conf. Electric Railways United Eur.*, 1995, pp. 131–135.
- [4] S. Chen and J. Rao, "Research on electromagnetic disturbance and its radiation level of an EMUs' traction inverter," in *Proc. 7th IEEE Int. Symp. Microw., Antenna, Propag., EMC Technol. (MAPE)*, Oct. 2017, pp. 252–255.
- [5] K. Sato, H. Kato, and T. Fukushima, "Development of SiC applied traction system for next-generation shinkansen high-speed trains," *IEEE J. Ind. Appl.*, vol. 9, no. 4, pp. 453–459, 2020.
- [6] K. Sato, H. Kato, and T. Fukushima, "Outstanding technical features of traction system in N700S shinkansen new generation standardized high speed train," *IEEE J. Ind. Appl.*, vol. 10, no. 4, pp. 402–410, 2021.
- [7] A. Mariscotti, "Critical review of EMC standards for the measurement of radiated electromagnetic emissions from transit line and rolling stock," *Energies*, vol. 14, no. 3, p. 759, Feb. 2021.
- [8] R. F. Gray and L. G. Ambrose, "EMI testing of a high speed rail train set," in *Proc. IEEE Symp. Electromagn. Compat.*, Chicago, IL, USA, Aug. 1994, pp. 242–247.
- [9] P. Pozzobon, A. Amendolara, B. Vittorini, U. Henning, R. Schmid, S. Shirran, and S. Ahlstedt, "Electromagnetic compatibility of advanced rail transport signalling," in *Proc. WCRR*, Edinburgh, U.K., 2003, pp. 1250–1263.
- [10] A. Morant, Å. Wisten, D. Galar, U. Kumar, and S. Niska, "Railway EMI impact on train operation and environment," in *Proc. Int. Symp. Electromagn. Compat. (EMC Europe)*, Rome, Italy, Sep. 2012, pp. 1–7.
- [11] E. J. Lombardi, "Engineering tests performed on the X2000 and ICE high speed trainsets," in *Proc. IEEE/ASME Joint Railroad Conf.*, Chicago, IL, USA, Mar. 1994, pp. 13–21.
- [12] E. Karadimou and R. Armstrong, "Test of rolling stock electromagnetic compatibility for cross-domain interoperability," *IET Intell. Transport Syst.*, vol. 10, no. 1, pp. 6–10, 2016.
- [13] R. D. Persichini, D. Di Febo, V. Cala, C. Malta, and A. Orlandi, "EMC analysis of axle counters in the Italian railway network," *IEEE Trans. Electromagn. Compat.*, vol. 57, no. 1, pp. 44–51, Feb. 2015.
- [14] A. Bialon, D. Adamski, and J. Furman, "Unified verification method of electromagnetic compatibility between rolling stock and train detection systems," *Sci. Trans. Prog. Bull. Dnipropetrovsk Nat. Univ. Railway Transp.*, vol. 63, no. 3, pp. 20–27, May 2021.
- [15] D. Mansson, R. Thottappillil, M. Backstrom, and O. Lunden, "Vulnerability of European rail traffic management system to radiated intentional EMI," *IEEE Trans. Electromagn. Compat.*, vol. 50, no. 1, pp. 101–109, Feb. 2008.
- [16] S. Midya and R. Thottappillil, "An overview of electromagnetic compatibility challenges in European rail traffic management system," *Transp. Res. C, Emerg. Technol.*, vol. 16, no. 5, pp. 515–534, Oct. 2008.
- [17] E. Karadimou, R. Armstrong, I. Adin, V. Deniau, J. Rodriguez, D. Galar, S. Niska, and J. Tamarit, "An EMC study on the interoperability of the European railway network," in *Proc. IEEE Int. Symp. Electromagn. Compat. (EMC)*, Dresden, Germany, Aug. 2015, pp. 428–433.
- [18] M. Miyachi, "The development of the speed verification type ATS with the transponder," *Quart. Rep. RTRI*, vol. 29, no. 3, pp. 103–106, Aug. 1988.
- [19] J. D. Portillo, M. Osinalde, E. Sukia, I. Sancho, J. Mendizabal, and J. Melendez, "Characterization of the EM environment of railway spot communication systems," in *Proc. IEEE Int. Symp. Electromagn. Compat.*, Detroit, MI, USA, Aug. 2008, pp. 1–6.
- [20] L. Xueming, Z. Ta, A. Ming, W. Lin, H. Guangzhong, and Z. Jianqiong, "Research on suppressing the interference of on-board BTM antenna by installing metal shielding plate," in *Proc. 5th Asia Conf. Energy Electr. Eng. (ACEEE)*, Kuala Lumpur, Malaysia, Jul. 2022, pp. 123–127.
- [21] Y. Balghithi, B. Meyniel, J. Orion, F. Maury, E. Francois, P. Besnier, and M. Drissi, "Proposa of a specific test methodology to assess the radiate immunity behavior of a data transmission from beacon to train," in *Proc. 20th Int. Zurich Symp. Electromagn. Compat.*, Zurich, Switzerland, Jan. 2009, pp. 485–488.
- [22] I. Watanabe and K. Ichikawa, "Effects of harmonics of VVVF controlled vehicles on signaling equipment," (in Japanese), *Railway Electr. Eng.*, vol. 6, no. 12, pp. 29–37, 1995.
- [23] M. Y. Joshi, G. Verma, R. G. Pawar, S. A. Walunj, S. M. Dagde, A. Dharan, C. V. Vinjuda, and S. R. Ranade, "Radiated emission measurements for MRVC II-electrical multiple unit (EMU) as per BS EN 50121-3-1:2006: A case study," in *Proc. 13th Int. Conf. Electromagn. Interference Compat. (INCEMIC)*, Visakhapatnam, India, Jul. 2015, pp. 74–76.
- [24] M. Y. Joshi, G. Verma, R. G. Pawar, S. M. Dagde, S. H. Solanki, A. Dharan, C. V. Vinjuda, L. Alex, and S. R. Ranade, "Radiated emissions measurement of entire railway system including rolling stock for Mumbai monorail project as per EN50121-2: A case study," in *Proc. 13th Int. Conf. Electromagn. Interference Compat. (INCEMIC)*, Visakhapatnam, India, Jul. 2015, pp. 77–80.
- [25] A. J. Rowell, D. Bozec, S. A. Sellar, L. M. McCormack, C. A. Marshman, and A. C. Marvin, "Improved measurement of radiated emissions from moving rail vehicles in the frequency range 9 kHz to 1 GHz," in *Proc. Int. Symp. Electromagn. Compat.*, Silicon Valley, CA, USA, Aug. 2004, pp. 19–24.
- [26] D. Bellan, A. Gaggelli, F. Maradei, A. Mariscotti, and S. A. Pignari, "Time-domain measurement and spectral analysis of nonstationary low-frequency magnetic-field emissions on board of rolling stock," *IEEE Trans. Electromagn. Compat.*, vol. 46, no. 1, pp. 12–23, Feb. 2004.
- [27] A. Mauriello and J. Clarke, "Measurement and analysis of radiated electromagnetic emissions from rail-transit vehicles," *IEEE Trans. Electromagn. Compat.*, vol. EMC-25, no. 4, pp. 405–411, Nov. 1983.
- [28] S. Paolessa, W. Picariello, L. Bocciolini, C. Zappacosta, S. D. Pascoli, B. Tellini, and M. Macucci, "Analysis of the electromagnetic emission of a railway vehicle according to the EN 50121-3-1 standard: A case study," in *Proc. Int. Symp. Electromagn. Compat. (EMC Europe)*, Rome, Rome, Italy, Sep. 2020, pp. 1–6.
- [29] Y. Yudhistira, Y. Yoppy, E. Trivida, T. A. W. Wijanarko, H. W. Nugroho, and D. Mandaris, "Electromagnetic interference measurement for axle counters light rapid transit railway in Indonesia," *Int. J. Electr. Comput. Eng. (IJECE)*, vol. 12, no. 5, p. 4632, Oct. 2022.
- [30] V. Deniau, N. B. Slimen, S. Baranowski, H. Ouaddi, J. Rioult, and N. Dubalen, "Characterisation of the EM disturbances affecting the safety of the railway communication systems," in *Proc. IET Colloq. Rel. Electromagn. Syst.*, Paris, France, 2007, pp. 1–5.
- [31] C. Chen, "Characterizing the generation & coupling mechanisms of electromagnetic interference noise from an electric vehicle traction drive up to microwave frequencies," in *Proc. APEC. 15th Annu. IEEE Appl. Power Electron. Conf. Expo.*, New Orleans, LA, USA, Feb. 2000, pp. 1170–1176.
- [32] D. Bellan, G. Spadacini, E. Fedeli, and S. A. Pignari, "Space-frequency analysis and experimental measurement of magnetic field emissions radiated by high-speed railway systems," *IEEE Trans. Electromagn. Compat.*, vol. 55, no. 6, pp. 1031–1042, Dec. 2013.
- [33] D. Valderas, I. Mesa, I. Adín, H. Lehmann, G. Lancaster, O. Stark, W. Baldauf, and J. del Portillo, "Modeling eddy current brake emissions for electromagnetic compatibility with signaling devices in high-speed railways," *IEEE Trans. Veh. Technol.*, vol. 66, no. 11, pp. 9743–9752, Nov. 2017.
- [34] Y. H. Wen and J. B. Zhang, "Statistical analysis on EMI to vehicular signaling system in CRH," in *Proc. Int. Conf. Electromagn. Adv. Appl. (ICEAA)*, Sep. 2016, pp. 541–545.
- [35] Y. Wen and W. Hou, "Research on electromagnetic compatibility of Chinese high speed railway system," *Chin. J. Electron.*, vol. 29, no. 1, pp. 16–21, Jan. 2020.
- [36] J. B. H. Slama and D. Chariag, "Measurement and analysis of magnetic field radiated from D.C. tramway: A case study for Tunis's metro," *J. Electr. Syst.*, vol. 4, no. 2, pp. 201–212, 2008.
- [37] M. N. Halgamuge, C. D. Abeyrathne, and P. Mendis, "Measurement and analysis of electromagnetic fields from trams, trains and hybrid cars," *Radiat. Protection Dosimetry*, vol. 141, no. 3, pp. 255–268, Oct. 2010.

- [38] S. Niska, "Measurements and analysis of electromagnetic interferences in the Swedish railway systems," Ph.D. dissertation, Luleå Railway Res. Centre, Univ. Tech. Luleå, Luleå, Sweden, 2008.
- [39] K. Jia, "High frequency model of electrified railway propulsion system for EMC analysis," Ph.D. dissertation, Div. Elec. Eng., KTH School Elec. Eng., Stockholm, Sweden, 2012.
- [40] C. Place, "Signalling and telecommunication compatibility issues," in *Proc. IET 13th Professional Develop. Course Electr. Traction Syst.*, vol. 690, 2014, pp. 199–212.
- [41] M. Heddebaut, V. Deniau, J. Rioult, and C. Gransart, "Mitigation techniques to reduce the vulnerability of railway signaling to radiated intentional EMI emitted from a train," *IEEE Trans. Electromagn. Compat.*, vol. 59, no. 3, pp. 845–852, Jun. 2017.
- [42] S. Azuma, D. Itoh, and K. Sugahara, "Reduction of return current noise using double-series resonant filter," *IEEJ Trans. Ind. Appl.*, vol. 129, no. 4, pp. 399–405, 2009.
- [43] S. Azuma, D. Itoh, T. Ishida, A. Iwata, K. Sugahara, and S. Morimoto, "Reduction of AM radio noise of a VVVF inverter for an electric railway car and simulation model of noise current," (in Japanese), *IEEJ Trans. IA*, vol. 139, no. 5, pp. 495–502, 2019.
- [44] S. Takahashi, K. Wada, H. Ayano, S. Ogasawara, and T. Shimizu, "Review of modeling and suppression techniques for electromagnetic interference in power conversion systems," *IEEJ J. Ind. Appl.*, vol. 11, no. 1, pp. 7–19, 2022.
- [45] S. Hatsukade and K. Wada, "Estimation of number of cores for preventing common-mode inductor saturation in railway traction inverters," *IEEE Access*, vol. 11, pp. 20418–20425, 2023.
- [46] P. Kirawanich, "An emission management framework for implementing a large railway system with interface complexity," *IEEE Electromagn. Compat. Mag.*, vol. 7, no. 2, pp. 54–63, 2nd Quart., 2018.
- [47] D. A. Leeming, J. Allan, and B. Mellitt, "Electromagnetic compatibility on rapid transit railways—A systems approach," in *Proc. 8th Int. Con. Electromagn. Compat.*, Edinburgh, U.K., 1992, pp. 227–234.
- [48] C. Place and D. Hayes, "Managing rolling stock EMC," in *Proc. IET Seminar EMC Railways*, London, U.K., Feb. 2009, pp. 1–8.
- [49] K. Matsushima, U. Paoletti, and K. Fukumasu, "Simulation method for inverter common-mode noise at the whole train level," in *Proc. Int. Symp. Electromagn. Compat. (EMC Europe)*, Rome, Italy, Sep. 2020, pp. 1–5.
- [50] K. Fukumasu, M. Nunokawa, U. Paoletti, K. Matsushima, and T. Takami, "Analysis method for magnetic field strength on on-board antenna due to inverter common-mode noise at whole train level," in *Proc. Int. Symp. Electromagn. Compat. (EMC Europe)*, Krakow, Poland, Sep. 2023, pp. 1–6.
- [51] S. Hatsukade and A. Yamanaka, "Calculation of interference between railway traction inverters and balises," in *Proc. Int. Symp. Electromagn. Compat.*, Tokyo, Japan, May 2014, pp. 65–68.
- [52] S. Hatsukade and A. Yamanaka, "Development of a pre-test for radiative emission from railway traction inverters," *IEEJ Trans. Ind. Appl.*, vol. 138, no. 10, pp. 766–776, 2018.
- [53] B. Audone, A. Gaggelli, P. Masini, and S. Neri, "Accreditation of radiated emission tests performed on train and complete vehicle," in *Proc. Int. Symp. Electromagn. Compat. (EMC Europe)*, Hamburg, Germany, Sep. 2008, pp. 1–6.
- [54] H. Elias, N. Perez, and H. Hirsch, "Experimental prediction of the radiated emission and final measurement process optimization based on deep neural networks according to EN 55032," in *Proc. Int. Symp. Electromagn. Compat. (EMC Europe)*, Gothenburg, Sweden, Sep. 2022, pp. 708–713.
- [55] H. Arai et al., "Development of detecting ATS beacons using spread spectrum method," (in Japanese), in *Proc. Railway Cybern. Symp.*, Tokyo, Japan, vol. 628, 2006, pp. 1–4.
- [56] Information and Communications Technology Subcommittee, Information and Communications Council. (Jul. 6, 2015). *Draft Report of the Radio Frequency Usage Environment Committee*. Accessed: Oct. 18, 2023. [Online]. Available: https://www.soumu.go.jp/main_content/000367149.pdf
- [57] *OpenTHFD*. Accessed: Oct. 18, 2023. [Online]. Available: <http://emoss.starfree.jp/OpenTHFD/index.html>
- [58] S. Hatsukade and K. Wada, "Octal-input zero-span-mode analyzer using FPGA boards," in *Proc. EMC+SIPI*, to be published.



SATORU HATSUKADE (Member, IEEE) was born in Tokyo, Japan. He received the B.S. and M.S. degrees in electronics engineering from The University of Tokyo, Japan, in 1994 and 1996, respectively. He is currently pursuing the Ph.D. degree in electrical engineering with Tokyo Metropolitan University, Tokyo.

Since 1996, he has been with the Railway Technical Research Institute, Tokyo. His current interests include research and development for electromagnetic interference between rolling stock and railway signaling systems. Furthermore, he provides expert consultation on electrical malfunctions of rolling stock and actively participates in various IEC standard maintenance teams.



KEIJI WADA (Senior Member, IEEE) was born in Hokkaido, Japan. He received the Ph.D. degree in electrical engineering from Okayama University, Okayama, Japan, in 2000.

In 2000, he was a Research Associate and an Associate Professor with Tokyo Metropolitan University, Tokyo, Japan, and Tokyo Institute of Technology. He has been a Professor with Tokyo Metropolitan University, since 2021. His current research interests include medium-voltage inverters, electromagnetic interference filters, and active power filters.

• • •